Progress In Electromagnetics Research C, Vol. 14, 131–145, 2010

A MINIATURIZED OPEN-LOOP RESONATOR FILTER CONSTRUCTED WITH FLOATING PLATE OVERLAYS

C.-Y. Hsiao

Institute of Electronics Engineering
National Tsing Hua University
No. 101, Section 2, Kuang-Fu Road, Hsinchu 300, Taiwan, R.O.C.

Y.-C. Chiang

Institute of Electronics Engineering
Chang Gung University
No. 259, Wen-Hwa 1st Road, Kwei-Shan
Tao-Yuan 333, Taiwan, R.O.C.

Abstract—This work presents a new technique that uses floating plate overlays to create an open-loop resonator bandpass filter characterized by a compact size and four controllable transmission zeros to achieve multispurious suppression. Three floating plate overlays are used to cover parts of the open-loop resonator filter to increase the coupling between resonators and move the transmission zeros to the desired frequencies to enhance harmonic suppression. A design procedure developed based on an equivalent circuit model of such new type of filter is proposed. Two experimental prototypes are designed and fabricated to verify the proposed design method. The measured results agree well with the simulations. The measured insertion losses of the prototypes in the passband are all less than 2 dB. One prototype is designed to suppress the third, fourth, and fifth harmonics with suppression greater than 30 dBc. Another prototype can suppress second, third, and fourth order harmonics below 20 dBc. In addition, the prototype circuit areas are only about 50% of the conventional open-loop filter.

Corresponding author: Y.-C. Chiang (ycchiang@mail.cgu.edu.tw).

1. INTRODUCTION

Microwave bandpass filters are widely used in commercial wireless communication systems. To satisfy the requirements of the modern communication system, the filter must be compact in size and have low insertion-loss in the desired passband and high attenuations in the stop-bands. Moreover, bandpass filters in the modern digital communication system are examined not only through their pass-band characteristics but also through their high-order harmonic suppressions. The open-loop resonator bandpass filter first proposed by Hong in 1995 [1] has been widely used in many microwave integrated circuits and wireless systems. The open-loop resonator filter is constructed by placing the half wavelength microstrip lines implemented by an open-loop shape with a certain coupling structure to achieve the requested filter performance. Three major types of coupling methods, electronic coupling, magnetic coupling, and mixed coupling structures, are used to create the filter with desired characteristics. Several design techniques have been reported [2–6] to minimize the size of a microstrip filter or suppress the spurious responses. One of these methods, the structure with capacitive terminations and 0° feeding structure (Fig. 1), has been shown not only to reduce filter size but also to shift the second pass-band to higher frequency to extend the bandwidth of the stop-band [3]. Recently, the effect of capacitive coupling caused by open-loop resonator ends has been analyzed to show that higher multispurious suppression can be achieved with higher coupling capacitance associated with open-loop resonator ends [7]. A circuit adopts the structure of the floating plate overlays to effectively increase the capacitive coupling between the microstrip lines for wideband application [8].

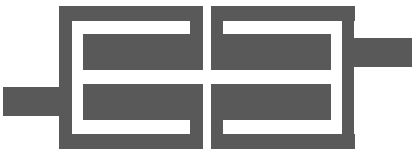

Figure 1. Structure of an open-loop resonator filter with capacitive terminations and 0° feeding structure.

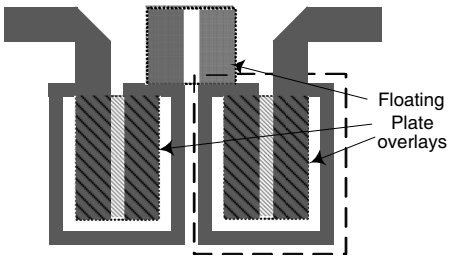

Figure 2. Open-loop resonator filter constructed with covering floating plate overlays.

In this paper, a new feature of the open-loop resonator filter constructed by placing floating plate overlays over the resonator capacitive terminations is proposed (Fig. 2) to further decrease the size of the open-loop filter and shift the second pass-band up to the sixth harmonic, resulting in a high multispurious suppression. The proposed filter structure can also provide a method to move the location of the transmission zero close to the higher passband corner. The structure in Fig. 2 shows the three floating plate overlays. Two of these, which are represented by oblique-line squares, are overlaid on the capacitive terminations of the conventional open-loop resonators. These floating plate overlays are produced by adhering upside-down PCBs, which are very thin and blank on one side, on the top metal of the PCB substrate.

Due to the compact size of the resonators of the proposed filter structure, conventional coupling methods used by the open-loop filter cannot achieve the desired characteristics in the pass-band. Thus, another floating plate overlay is used to increase the capacitive coupling between the resonators to achieve the desired pass-band characteristics. The following section proposes an equivalent circuit model associated with such an open loop filter to analyze the characteristics of the filter. After determining how the components of the filter affect the characteristics of the filter from the previously obtained results, a procedure of the proposed filter feature is designed. Such a procedure, which includes short-circuit stubs to realize a transmission zero at the lower stop-band to increase the required attenuation, is proposed in Section 3. Meanwhile, the designs and measurements of the two experimental prototypes are described in Section 4. Measurement results agree well with the theoretical predictions and EM-simulations. The size of the prototypes is very compact compared with that of the conventional open-loop resonator filter with capacitive terminations and is only about 50% of the size of the conventional filter.

2. ANALYSIS OF THE FILTER CONSISTING OF AN OPEN-LOOP RESONATOR WITH FLOATING PLATE OVERLAYS

To analyze the circuit structure (Fig. 2), an equivalent circuit model composed of lumped elements (Fig. 3) is proposed. The circuitry of a single resonator enclosed by the dotted line square (Fig. 2) and comprised of C_1, C_2, L_1, and L_2 (Fig. 3) is first studied. The admittance matrix of such a single resonator can be obtained as follows:

$$\begin{bmatrix} Y_{11} & Y_{12} \\ Y_{21} & Y_{22} \end{bmatrix}_r = \begin{bmatrix} g+h & -g \\ -g & g+h \end{bmatrix} \tag{1}$$

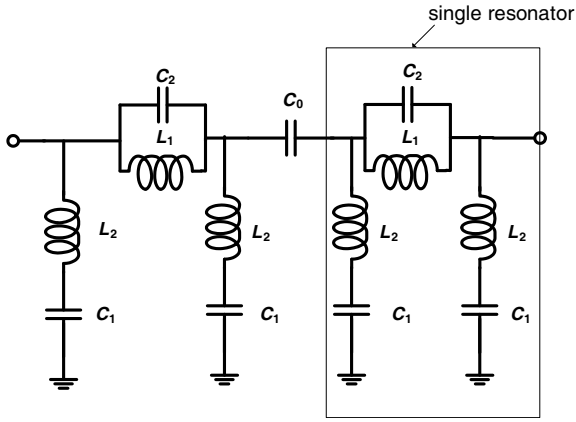

Figure 3. Equivalent circuit model of an open-loop resonator filter covered with floating plate overlays.

where

$$g = j\omega C_2 + 1/(j\omega L_1) \tag{2}$$

and

$$h = j\omega C_1 / \left(1 - \omega^2 L_2 C_1\right). \tag{3}$$

By checking the frequency response of the single resonator, such a circuit is found to be a wide-band notch filter with two transmission zeros (f_{z1} and f_{z2}) in the stop-band given by

$$f_{z1} = 1/2\pi(C_2 L_1)^{1/2} \tag{4}$$

and

$$f_{z2} = 1/2\pi(C_1 L_2)^{1/2}. \tag{5}$$

Lower and higher corner frequencies (f_{c1} and f_{c2}) of pass-bands are given by

$$f_{c1} = \sqrt{\frac{R_a - R_c}{R_b}}/2\pi \tag{6}$$

and

$$f_{c2} = \sqrt{\frac{R_a + R_c}{R_b}}/2\pi, \tag{7}$$

respectively, where

$$R_a = L_1 C_2 + C_1 L_2 + (C_1 L_1)/2, \tag{8}$$

$$R_b = 2L_1 L_2 C_1 C_2, \tag{9}$$

and

$$R_c = \sqrt{R_a^2 - 2R_b}. \tag{10}$$

Comparing the equivalent circuit model with the structure of the resonator (Fig. 2), C_1 is found to correspond with the shunt capacitor used as capacitive termination in the conventional design. C_2 represents the capacitive coupling between microstrip stubs caused by the floating plate. As the floating plate is much thinner than that of the substrate, the capacitance of C_2 should be much greater than C_1. According to (4) and (6), the filter constructed by adopting the floating plate overlays can dramatically decrease lower pass-band corner frequency and increase one more transmission zero, thereby reducing the circuit size of the filter and enhancing the attenuation in the upper stop-band.

Figure 4 compares the simulated frequency responses of the equivalent circuit model and the EM simulation of a resonator fabricated on an FR4 PCB substrate; the ground of the structure is on the reverse side of the PCB substrate. Both are quite similar, which demonstrates the proposed equivalent circuit model can be effectively approximate to such a resonator. The overall characteristics of the filter in Fig. 3 can be obtained by cascading the transmission matrices of the resonators and the coupling capacitor as follows:

$$\begin{bmatrix} A & B \\ C & D \end{bmatrix}_{total} = \begin{bmatrix} A & B \\ C & D \end{bmatrix}_r \times \begin{bmatrix} A & B \\ C & D \end{bmatrix}_c \times \begin{bmatrix} A & B \\ C & D \end{bmatrix}_r \tag{11}$$

where the transmission matrices of the single resonator and series-

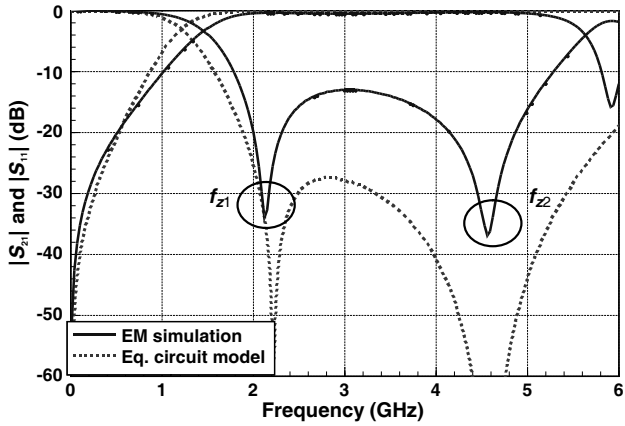

Figure 4. Comparison of S_{21} and S_{11} of the EM simulation of a single resonator and the equivalent-circuit model.

connected capacitor (C_0) are given by

$$\begin{bmatrix} A & B \\ C & D \end{bmatrix}_r = \begin{bmatrix} 1 + h/g & 1/g \\ 2 \times h + h^2/g & 1 + h/g \end{bmatrix} \tag{12}$$

and

$$\begin{bmatrix} A & B \\ C & D \end{bmatrix}_C = \begin{bmatrix} 1 & 1/(j\omega C_0) \\ 0 & 1 \end{bmatrix}, \tag{13}$$

respectively. Applying the well-known transfer method [9], the transmission matrix of (11) can be transferred to the S parameter matrix representing the S parameters (S_{11} and S_{21}) of the filter. Fig. 5 shows the filters consisting of different coupling capacitors C_0 but with the same resonator structure. Such a condition depicts the filters all exhibiting second-order band-pass with two different transmission poles, represented by f_{p1} and f_{p2} in the pass-band (Fig. 5), while the filter consists of different coupling capacitors. Frequencies of these transmission poles can be obtained by solving the equation $S_{11} = 0$, where S_{11} is the first row and first column element of the S parameter matrix transferred from Eq. (11). Fig. 5 also shows that the transmission pole near the higher pass-band corner (f_{p2}) is always located at about $\sqrt{2}f_{c1}$ of the filter constructed with different coupled capacitors, as the location of f_{p2} is determined by the single resonator structure. The coupling capacitor effect moves the location of f_{p1} to lower frequency, while the filter consists of a higher capacitance of C_0. Fig. 6 compares the frequency responses of the single resonator and the whole filter, showing that the transmission zero locations of the single resonator and band-pass filter are almost the same, and that the second passband of the band-pass filter is similar to the higher pass-band corner of the single resonator.

Although the proposed filter feature adopts a strong capacitive coupling feature to implement the required pass-band characteristics, the layout of the proposed filter still belongs to the type of mixed coupling structure. The weak inductive coupling between the two resonators causes one more transmission zero close to the higher passband corner and pushes the transmission zero (f_{z1}) to a higher frequency. Such characteristics can be obtained (Fig. 7) by assuming only the adjacent inductors L_2 in Fig. 3 with coupling coefficients of 0.01–0.03 between them. Fig. 7 depicts the EM simulation results of the filters constructed with different separation distances between the two resonators and the resonators of filters with similar layout structures and connected to the ideal coupling capacitor with the same capacitance. In Fig. 7, d_a, d_b, and d_c are the separations between the resonators adopted by three different filters and $d_c > d_b > d_a$.

Figure 7 shows that the locations of the three transmission zeros in the upper stop-band vary when the layout of the filter adopts a different separation. It also shows that with smaller separation, the location of the transmission zero is closer to the higher passband corner. Based on Fig. 7, the incremental transmission zero caused by the inductive coupling between inductors l_2 should be the one closest to the pass-band corner because the location of the next transmission zero moves back to the original location of f_{z1} as the resonators are separated widely.

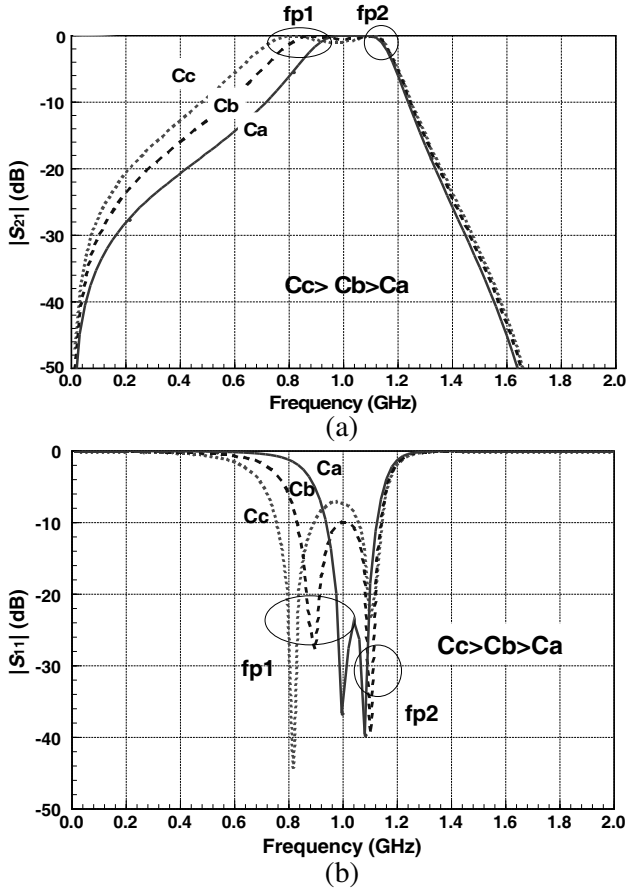

Figure 5. (a) Simulated S_{21} of the filters constructed with resonators consisting of the same elements but using different values of coupling capacitors (C_0), where C_a, C_b, and C_c represent the different capacitive values of C_0 and $C_c > C_b > C_a$. (b) S_{11} of the filters constructed by adopting different values of coupling capacitors (C_0).

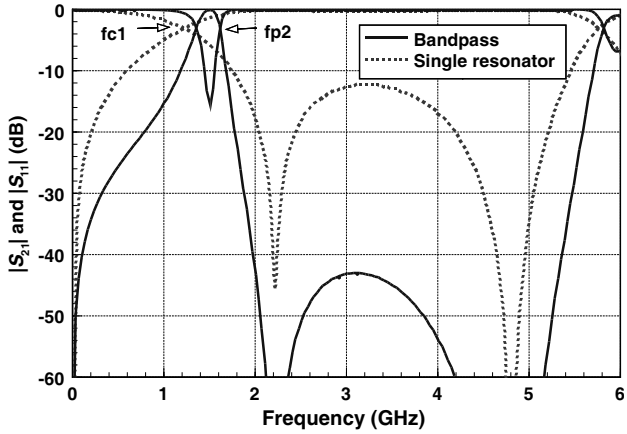

Figure 6. Comparison of S_{21} and S_{11} of the single resonator and bandpass filter.

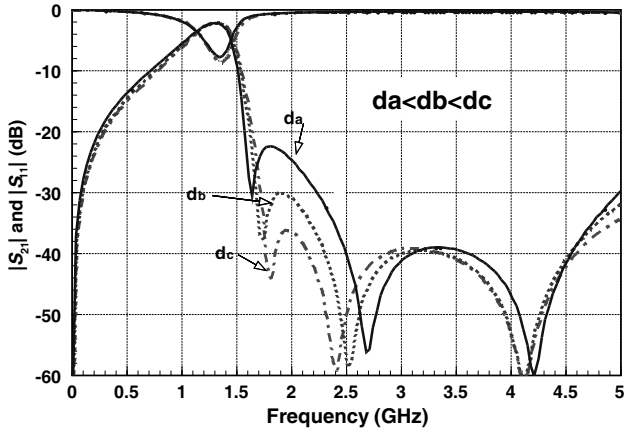

Figure 7. S_{21} and S_{11} of the filter with different separation distances between two resonators.

3. DESIGN OF AN OPEN-LOOP FILTER WITH FLOATING-PLATE OVERLAYS

Based on the results obtained in the previous section, a procedure for designing the open-loop filter with floating plate overlays is suggested to determine the appropriate physical layout pattern (Fig. 8) according to the given filter specifications:

1) The physical layout of the single open-loop resonator with floating plate overlay should be determined first to possess the following notch filtering characteristics. The lower pass-band corner frequency (f_{c1}) in the lower pass-band is located at about $0.707f_{p2}$. The higher pass-band corner is located at six times of f_0, where f_0 is the central frequency of the bandpass filter, and f_{p2} is equal to the higher pass-band corner frequency. The location of the second transmission zero (f_{z2}) is about five times of f_0 to better obtain an achievable multispurious suppression. The location of the first transmission zero is about twice the difference between the specified transmission zero frequency and the passband corner of the band-pass filter away from the higher pass-band corner. The equivalent-circuit model element values are extracted after the resonator layout is determined (Fig. 3), corresponding to such a layout pattern.
2) Bringing the values of the equivalent model of the obtained elements (12) and cascading the coupling capacitor transmission matrix with unknown capacitance can obtain S parameters of the filter with only one unknown value C_0. The coupling capacitor (C_0) value can be determined by solving the equation $S_{11} = 0$ according to the required pass-band bandwidth. The appropriate layout for achieving C_0 corresponding to the value of G_1 (Fig. 8) can then be determined. Otherwise, the different values of C_0 can be obtained by simply adjusting the length of l_7 (Fig. 8).

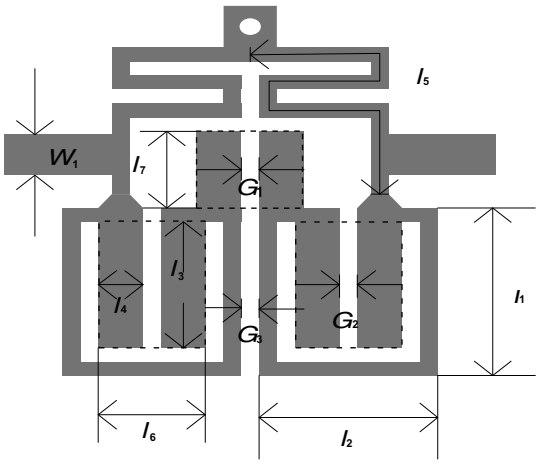

Figure 8. Overall physical layout of an open-loop resonator filter constructed with floating plate overlays and short-circuit stubs.

3) Deciding the physical layout of the resonators and coupling capacitor can then be analyzed to verify whether the attenuation in the higher stop-band can satisfy the specified characteristics. If the characteristics of the filter cannot satisfy the required specifications, the designer can slightly adjust the separation between the resonators, represented as G_3 (Fig. 8), to vary the transmission zero locations.
4) Figure 7 shows that the attenuation in the lower stop-band is

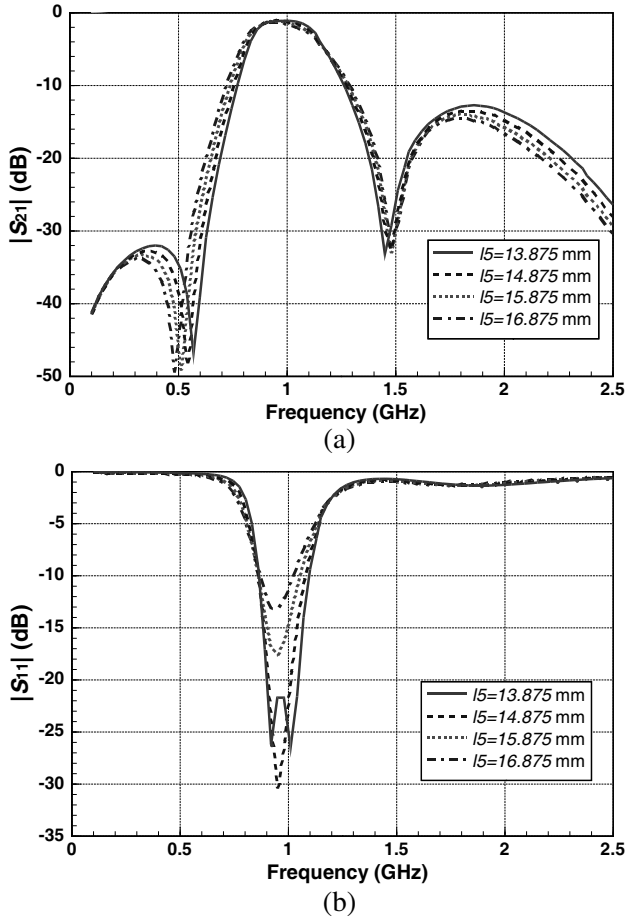

Figure 9. (a) S_{21} of filters constructed with different lengths of short-circuit stubs (l_5). (b) S_{11} of filters constructed with different lengths of short-circuit stubs (l_5).

not so good. One method that adopts the short-circuit stubs (Fig. 8) may be used to improve the attenuation of the lower stop-band [10]. The short-circuit stubs have very weak influence in the pass- and higher stop-band when the resulting transmission zero is not very close to the pass-band corner, such that these short-circuit stubs can be directly connected to the previously obtained layout of the filter. The transmission zero location at the lower stop-band is controlled by adjusting length l_5 (Fig. 8). The responses are almost the same as those in the region of the pass- and higher stop-band (Fig. 9), but the locations of the transmission zeros at the lower stop-band shift when the filter is constructed with different short-circuit stub lengths.

4. DESIGNS AND MEASUREMENTS OF THE FILTER PROTOTYPES

Two prototypes of the proposed filter structure are designed and fabricated to verify the design concept. The substrate used for implementing the experimental filters and all the floating plate overlays is FR4 PCB with a relative dielectric constant of $\varepsilon_r = 4.3$ and a loss tangent of 0.02. Note that the loss tangent of FR4 PCB given by manufacture is measured at hundred mega hertz. However, it is found that the loss tangent provided by the FR4 manufacture still shows quite good correspondence with the experimental result for the circuits operated below 4 GHz in our own experiences and almost independent of frequency. Therefore, the dielectric loss of the FR4 PCB results in the increasing of the insertion losses in the passband, and there is no influence in the bandwidth of passband and positions of transmission zeros, while the operation frequencies are below 4 GHz. However, the dielectric loss will be increased after the operation frequencies above 4 GHz that not only results in higher insertion loss, but also causes moving positions of transmission zeros as that shown in the measurement results. Besides, the dielectric loss of the FR4 substrate lowers the quality factors of the components fabricated on the FR4 substrate. Thus, a filter designer wants to minimize the insertion loss in the passband or achieve the passband width narrower than the proposed prototype. He can fabricate the filter with selecting Teflon or Duroid® substrates instead of using FR4 PCB. The substrate thickness and dielectric layer supporting the floating plate overlays are 0.75 and 0.138 mm, respectively. The surrounding of the simulation is a close conductor, and the distance between the conductor and filter is 1.35 mm.

The physical layout of the single resonator having band-stop

characteristics described in the previous section is first determined. The element values of the equivalent circuit model associated with such a layout pattern are extracted to be $C_0 = 0.3\,\text{pF}$, $C_1 = 0.42\,\text{pF}$, $C_2 = 0.5\,\text{pF}$, $L_1 = 10.3\,\text{nH}$ and $L_2 = 2.64\,\text{nH}$. Fig. 10 shows the photograph of the prototype. W_1 is identical to the width of a $50\,\Omega$ microstrip line. The practical dimensions of the layout pattern of the filter corresponding to that in Fig. 8 are $W_1 = 1.45\,\text{mm}$, $l_1 = 6\,\text{mm}$, $l_2 = 5\,\text{mm}$, $l_3 = 4.5\,\text{mm}$, $l_4 = 1.25\,\text{mm}$, $l_5 = 13.9\,\text{mm}$, $l_6 = 3\,\text{mm}$, $l_7 = 2.75\,\text{mm}$, $G_1 = 0.5\,\text{mm}$, $G_2 = 0.5\,\text{mm}$, and $G_3 = 0.5\,\text{mm}$. With adopting $l_5 = 13.9\,\text{mm}$ to fabricate the experimental prototype, the filter can achieve fast roll off in the lower stop band. It is shown in Figs. 9(a) and (b) that the location of the transmission zero in lower stop band is completely determined by the length of l_5, and the shorter length of l_5 is the higher frequency of the transmission zero at low stop band is obtained. Actually, the length of l_5 in the practical application should be determined according to the required rejection given by the specifics of the wireless communication system. Total filter size is approximately $10.5\,\text{mm} \times 13.2\,\text{mm}$, which is equivalent to $0.03\lambda_g \times 0.033\lambda_g$, where λ_g is the propagation wavelength of a $50\,\Omega$ transmission line fabricated on the same FR4 substrate.

S-parameters of the prototypes are measured by the HP8753D network analyzer. Fig. 11 illustrates the measured and simulated S_{21} and S_{11} of the prototype in Fig. 10. The center frequency of the prototype is about 1 GHz. Fractional bandwidth of the filter is about 20%. Insertion losses in the pass-band are less than 2.0 dB associated with greater 13 dB return loss; the attenuation at the region below 0.62 GHz is higher than 30 dB; and the attenuation of the higher stop-band is greater than 20 dB in the 2.5–5.4 GHz region. Three transmission zeros located at 1.55, 3.2, and 4.66 GHz are achieved to effectively suppress the third, fourth, and fifth harmonics up to 30 dB.

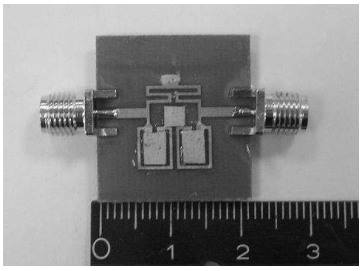

Figure 10. Photograph of a miniaturized open-loop resonator filter constructed on FR4 PCB.

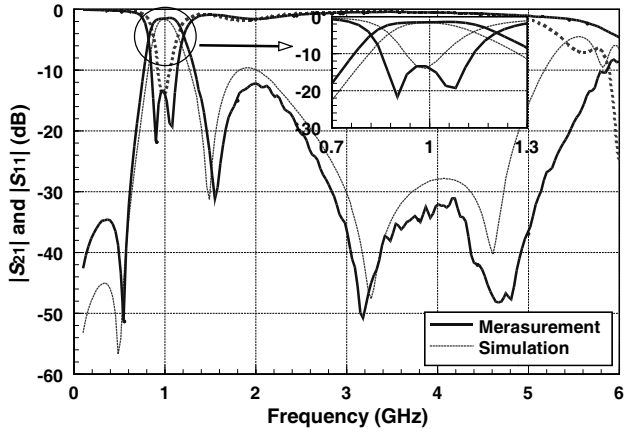

Figure 11. Measured and simulated S_{21} and S_{11} of the filter prototype in Fig. 10.

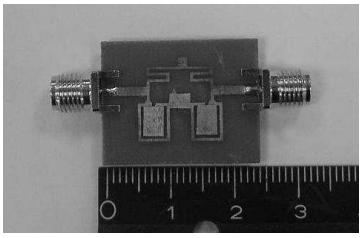

Figure 12. Photograph of the second prototype constructed on FR4 PCB.

According to Fig. 7, better suppression can be obtained in the second harmonic by increasing the separation between resonators.

Therefore, another prototype constructed with the gap (G_3) of 3.25 mm while keeping the other parameters the same is fabricated. Fig. 12 shows the photograph of the prototype created with a separation between resonators larger than the previous one. The measured and simulated S-parameters of the second prototype are illustrated in Fig. 13, which shows that the second harmonic can be suppressed up to 20 dB while the first transmission zero at a higher stop-band is moved to 1.6 GHz. However, the suppressions of the third and fourth harmonics can only be greater than 20 dB, which is worse than the previous one.

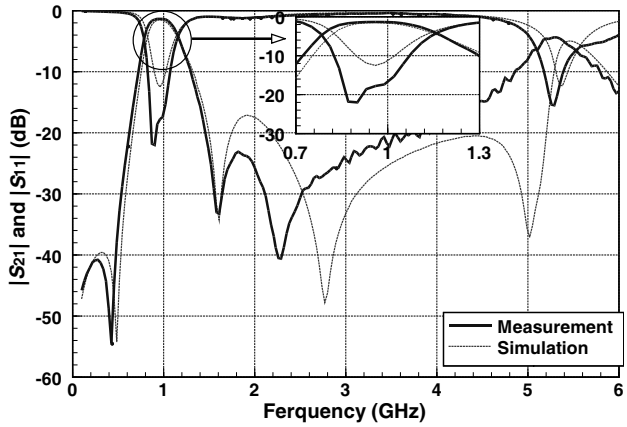

Figure 13. Measured and simulated S_{21} and S_{11} of the filter in Fig. 12.

5. CONCLUSION

This work presents a new configuration of a microwave filter constructed by covering floating plate overlays over parts of a conventional open-loop resonator filter. This new filter feature has the advantage of reduced size, resulting in multiple transmission zeros to enhance suppressions of high-order harmonics. A filter design procedure, which can effectively obtain the desired passband characteristics and controllable transmission zeros located at higher and lower stop-bands, respectively, is described. Two experimental filters are designed and fabricated to verify the proposed design method. The measurement results are close to the theoretical predictions. The proposed filter can save more than 50% of the circuit area compared with the conventional open-loop resonator filter with capacitive terminations. The results also demonstrate good characteristics in both pass- and stop-bands compared with the conventional designs.

ACKNOWLEDGMENT

This work was supported by the National Science Council of Taiwan, R.O.C., under Project NSC 96-2815-C-182-006-E.

REFERENCES

1. Hong, J. S. and M. J. Lancaster, "Canonical microstrip filter using square open-loop resonators," *IEE Electron. Let.*, Vol. 31, No. 23, 2020–2022, Nov. 1995.
2. Tsai, C. M., S. Y. Lee, and C. C. Tsai, "Performance of a planar filter using a 0° feed structure," *IEEE Microwave Theory and Techniques*, Vol. 50, No. 10, 2362–2367, Oct. 2002.
3. Gu, J. Z., F. Zhang, C. Wang, Z. Zhang, M. Qi, and X. W. Sun, "Miniaturization and harmonic suppression open-loop resonator bandpass filter with capacitive terminations," *IEEE Microwave Symposium Digest*, 373–376, Jun. 2006.
4. Hong, J. S., "Dual-mode microstrip open-loop resonator and filters," *IEEE Microwave Theory and Techniques*, Vol. 55, No. 8, 1764–1770, Aug. 2007.
5. Chin, K. S. and D. J. Chen, "Novel microstrip bandpass filters using direct-coupled triangular stepped-impedance resonators for spurious suppression," *Progress In Electromagnetics Research Letters*, Vol. 12, 11–20, 2009.
6. Chin, K. S. and C. K. Lung, "Miniaturized microstrip dual-band bandstop filters using tri-section stepped-impedance resonators," *Progress In Electromagnetics Research C*, Vol. 10, 37–48, 2009.
7. Chin, K. S., Y. C. Chiang, and J. T. Kuo, "Microstrip open-loop resonator with multispurious suppression," *IEEE Microwave and Wireless Components Letters*, Vol. 17, No. 8, 574–576, Aug. 2007.
8. Chiang, Y. C. and C. H. Hsieh, "Wideband microwave filter constructed by asymmetrical compact microstrip resonator and floating plate coupling structure," *IET Electronics Letters*, Vol. 43, No. 14, 762–763, Jul. 2007.
9. Pozar, D. M., *Microwave Engineering*, 3rd edition, John Wiley & Sons, 2005.
10. Chen, C. F., T. Y. Huang, and R. B. Wu, "A miniaturized net-type microstrip bandpass filter using $\lambda/8$ resonators," *IEEE Microwave and Wireless Components Letters*, Vol. 15, No. 7, 481–483, Jul. 2005.